Analyzing the Effects of Mercury on Acetylcholinesterase *In Vitro*

By Jessica Michelle Strange

APPROVED BY:

Jennifer F. Nyland, Ph.D., Advisor — 20 June 2022 — Date

Jessica K. Clark, Ph.D., Committee Member — 6/20/22 — Date

Jose I. Juncosa, Ph.D., Committee Member — 6/20/22 — Date

Dana L. Price, Ph.D., Graduate Program Director — 6/23/22 — Date

Analyzing the Effects of Mercury on Acetylcholinesterase *In Vitro*

By

Jessica Michelle Strange

A thesis submitted to the Department of Biological Sciences of Salisbury University in partial fulfillment of the requirements for the degree of

Master of Science Applied Biology

June, 24, 2022

Dedication

To Juniper Louise and John B. Fegan.

Without your support, I would never have made it this far.

In loving memory of

Peg Foster, "Hey, look mom, I made it"

&

Bobby Peek, "Dad, I did goodly."

Acknowledgments

I want to thank everyone who has been part of this journey, even if only for a moment. The influential staff and doctors at Chesapeake Eye Center who first inspired me to take this journey, Terry Thompson at Wor-Wic Community College for the unwavering belief in me from day one, My friends with the Baltimore Marching Ravens, the staff at Olive Garden who took an interest in making "Dr. Strange", Lela for being the ultimate hype man and best friend through thick and thin, Dave for being there for anything I needed, and every soul who played a part in my story. My family in Phi Theta Kappa whom I can't even begin to thank the support they continue to give; you all are everything. The friends who kept me grounded and reminded me it's ok to slow down and enjoy the process, the ones who I've said goodbye, and most importantly, the ones who inspire me to "leave it better than I found it."

Thank you to John and June for the sacrifices they have made through this journey. Time is irreplaceable, and both of you have allowed me to give this precious resource to the pursuit of science, higher education, and my goal of improving the world. Thank you even more for all the hugs, kisses, days on the playground, road trips, and dance breaks. The world is already better because you're in it and nothing makes me happier than being your mom and partner.

I would also like to acknowledge the other three leading ladies in this cohort, known simply as "The Exit Buddies" from Finding Nemo. Thank you, Sheridan, Emily, and Steph, for a level of comradery and absolute insanity I couldn't imagine living without. You all have made this journey during a global pandemic truly wonderful. I can't wait to watch your continued growth and contributions to society. To the rest of our biology cohort, the

TA support staff, and the department, you have also been amazing beyond measure and I'm fortunate beyond words to call you friends.

I would like to also thank my committee for everything. Thank you, Jose, for joining the team and keeping me inspired to love organic chemistry. That is a talent very few possess, but your love for teaching and passion for chemistry is nothing short of remarkable. Jessica, thank you for supporting my crazy idea and taking on Sheridan as a grad student so I could meet one of my favorite people. Between the two of you I have had so many laughs and an appreciation for *Danio rerio*. I hope you never forget how much of an impact you have on all your students, and you continue to inspire the next generation of biologists to change the world.

Jennifer F. Nyland, the woman who changed my life, perspective, and trajectory. There will never be an acknowledgment or "Thank you" conveying how grateful I am for you. I grew as a scientist, mother, and person because of your influence. Your knowledge and scientific abilities are inspiring, but your personality and talent for education are extraordinary. I could not have dreamed up a more perfect mentor for this journey. There aren't many people I can have a foot race through Henson with, supply fresh eggs (thanks Nessie and the rest of the crew), learn enzyme kinetics and statistics, laugh over black coffee, and enjoy every conversation. I am so excited to see what you do next because I'm sure it will be nothing short of epic. You are truly improving this rock floating through space, and I thank you for being part of my journey on it.

Table of Contents

Page

List of Tables

Page

List of Figures

Page

List of Abbreviations

ACh	acetylcholine
AChE	acetylcholinesterase
AChR	acetylcholine receptor
CAP	cholinergic anti-inflammatory pathway
DTNB	5,5-Dithiobis-(2-nitrobenzoic acid)
IFN	interferon
IL	interleukin
IP3	inositol triphosphate
JAK	Janus kinase
LPS	lipopolysaccharide
NF_KB	nuclear factor-kappa b
PAMP	pathogen-associated molecular patterns
PRR	pattern recognition receptor
STAT	signal transducer and activation of transcription
TLR	toll-like receptor
TNB	5-thio-2-nitrobezoate
TNF-α	tumor necrosis factor alpha

Abstract

This study aims to establish a viable method for testing the relationship between low doses of inorganic mercury and the enzyme acetylcholinesterase (AChE) *in vitro*. Mercury has been identified as a heavy metal that can induce an immune response through cytokine signaling, resulting in an unopposed inflammatory response by downregulating the production of anti-inflammatory cytokines. The ubiquity of mercury as an environmental toxicant and its ability to bioaccumulate and become biomagnified makes it a xenobiotic of interest in many toxicological studies. This is notably performed in concentrations of micromolar ranges or higher. Previous findings support a dysregulation of the immune response when mercury exposure occurring in the nanomolar range is coupled with bacterial or viral adjuncts. This co-exposure is demonstrated exasperating the effects seen in the inflammatory response through the inhibition of the anti-inflammatory counteraction of the immune system to reestablish homeostasis. The further understanding of the cholinergic anti-inflammatory pathway (CAP) and the enzyme AChE as a regulator is one area of interest when hypothesizing the mechanism of this inflammatory response. This research presented in this manuscript establishes the use of a continuous assay based on Ellman's method as a viable method to assess the effects of mercury on AChE *in vitro* which allows for the further analysis of this complex relationship between low dose mercury exposures, bacterial adjuncts, and the CAP. Specifically, this method offers an explanation for a potential mechanism of how these components relate to one another and the upregulation of the inflammatory response, and specifically how it becomes unchallenged.

Introduction

Mercury, in its various forms, is a ubiquitous environmental toxicant affecting populations and ecosystems worldwide at various concentrations. This heavy metal is non-essential for the functioning of the human body, and both chronic and acute exposures result in varying complications. This global toxicant occurs in a variety of different forms including elemental, organic, and inorganic. The toxicological effects of mercury on both the nervous system and the immune system can differ based on these different forms, different concentrations, and even other environmental co-exposures.

The elemental form of this xenobiotic is a liquid at room temperature and is commonly referred to as quicksilver due to its color and state of matter. Elemental mercury is found in items as common as old thermometers or electrical switches (U.S. Environmental Protection Agency, 2022b). The toxicological risks of this form are most dangerous through inhalation of the vapor rather than dermal absorption (Research Triangle Institute, 1999). Clinical presentations of toxicity resulting from elemental mercury exposures include various symptoms. These symptoms which include weakness, fatigue, anorexia, and gastrointestinal distress at chronic low doses. Coarse shaking, gingivitis, and excessive salivation have been reported at higher exposures (Berlin, Zalpus, & Fowler, 2007)

The inorganic form of mercury (iHg) is commonly joined with other elements. Mercuric salt compounds are notably found bonded to oxygen, chlorine, or sulfur (Research Triangle Institute, 1999). Inorganic mercury is widely found in waste from coal-fired power plants and used in vibrant tattoo ink colors, most notably red (U.S. Environmental Protection Agency, 2022b). Clinical presentations reported in mercuric

chloride ($HgCl_2$) exposures include bloody diarrhea, abdominal pain, and renal complications, which can be long-term (Berlin, Zalpus, & Fowler, 2007).

When the elements bonding with mercury contain a carbon grouping, the resulting compound is termed organic mercury. Organic mercury is most commonly found as an environmental toxicant in methyl and ethyl forms. Methylmercury is frequently found in predatory fish (U.S. Environmental Protection Agency, 2022b) and, due to its low polarity can cross both the blood-brain barrier causing neurological complications, and the placenta posing a substantial risk to the fetus in pregnancy. Clinical presentations of methylmercury exposures include loss of peripheral vision, decrease in coordination, and muscle weakness (U.S. Environmental Protection Agency, 2022a; National Research Council, 2000).

Mercury's definition as a global environmental toxicant is often associated with coastal environments. Aquatic environments and the water cycle play an essential role in the biogeochemical cycling of mercury. Both organic mercury and inorganic mercury are present in these environments (U.S. Environmental Protection Agency, 2022b; Li & Cai, 2013). Previous work has identified 200nM concentrations as physiologically relevant levels of exposure through normal environmental exposures. This concentration corresponds with previously identified levels of mercury found in the blood (37 ug/L) following environmental exposures to mercury. These exposure levels are within the ranges found in exposures in the U.S (Crompton et al., 2002; Hightower and Moore, 2003).

Bioaccumulation, biomagnification, and remobilization also contribute to mercury's role in the environment and toxicity as a result of exposure. As higher trophic level organisms consume lower trophic level organisms, the mercury that is not excreted from the lower-level organisms is accumulated and thus it is biomagnified up the food web

(Houserová et al., 2007, Skinner et al., 2007; Regiera et al., 2013). In addition to biomagnification and bioaccumulation, remobilization is a factor in increasing mercury's environmental presence. Remobilization occurs when the element is released from sediments and detritus and reenters the cycle. This is seen with factors such as wildfires (Tuhy et al., 2020).

An additional quality contributing to mercury's status as a global toxicant is its ability to be methylated and demethylated, which originates from both biotic and abiotic factors. The methylation of inorganic mercury through sulfate-reducing bacteria or chemicals such as low-weight organic acid is the primary source of environmental methylmercury. Opposite of methylation, demethylation occurs in sediment and periphyton (Li & Cai, 2013) and can occur in tissues *in situ* through demethylation enzymes.

These defining characteristics of this heavy metal and its movement in the aforementioned and other environmental settings increase risks for exposures at all trophic levels within food webs and in multiple environments. Of particular importance is the potential for mercury to bioaccumulate as it is not always readily excreted, notably in aquatic environments (Li & Cai, 2013). The process of bioaccumulation results in elevated mercury concentrations in higher trophic-level organisms such as large fish-eating aquatic life like tuna. Thus, consumption of contaminated fish at these higher trophic levels results in higher mercury exposure in apex predators including humans. Previous studies have demonstrated significant mercury exposure to riverside communities downstream of small-scale artisanal gold mining operations in Amazonian Brazil where elemental mercury is

used to extract small flecks of gold from river sediments (Silva et al., 2004, Gardner et al., 2010a).

Interestingly, other foods where biomagnification and higher trophic levels are not critical to dietary intake, there is the potential for these foods to serve as sources of mercury exposure through bioaccumulation. One food source constituting this type of documented exposure risk is rice, which results in human dietary exposure to methylmercury at levels comparable to that observed from contaminated fish consumption due to its important role in some diets (Rothenberg et al., 2016). Previous studies into how these exposures negatively impact the biological system overall require further investigation into the mechanics of the immune system prior to and in response to the exposure to mercury.

The primary purpose of the immune system is to protect organisms from foreign pathogens. There are two distinct branches of the immune system characterized by specificity of the response to these pathogens. The body's initial response is the innate immune system, which is not specific for particular pathogenic exposures, but rather, is based on broad molecular patterns and is highly conserved in mammals. The second branch is the adaptive immune response, which is specific to different pathogens and increases destruction effectiveness with each exposure to the same pathogen (Nathan et al.,1983; Stein et al., 1992). For the scope of this study, the innate immune system is the focus.

In the innate immune system, vital components include physical and chemical barriers, cellular components, and the humoral response. The part of this response of interest here is cellular components, specifically macrophages. Macrophages are derived from the myeloid lineage, which produce monocytes, macrophages, microglia, and dendritic cells. Peripheral macrophages are further classified by two distinct phenotypes.

The M1 type of macrophage is classically activated by the presence of lipopolysaccharide (LPS) or interferon gamma (IFN-γ) and characterized by the release of pro-inflammatory cytokines, most notably tumor necrosis factor alpha (TNF-α). These small proteins are used for chemical signaling and mobilizing the immune response against pathogens and tumors. The M2 phenotype macrophages are known as alternatively activated and are characterized by their release of anti-inflammatory cytokines. Additionally, macrophages can become polarized to different phenotypes based on different stimulants. The ability to change between the different phenotypes is termed macrophage plasticity (Yaun et al., 2014; Wongtrakool et al., 2012) (Figure 1).

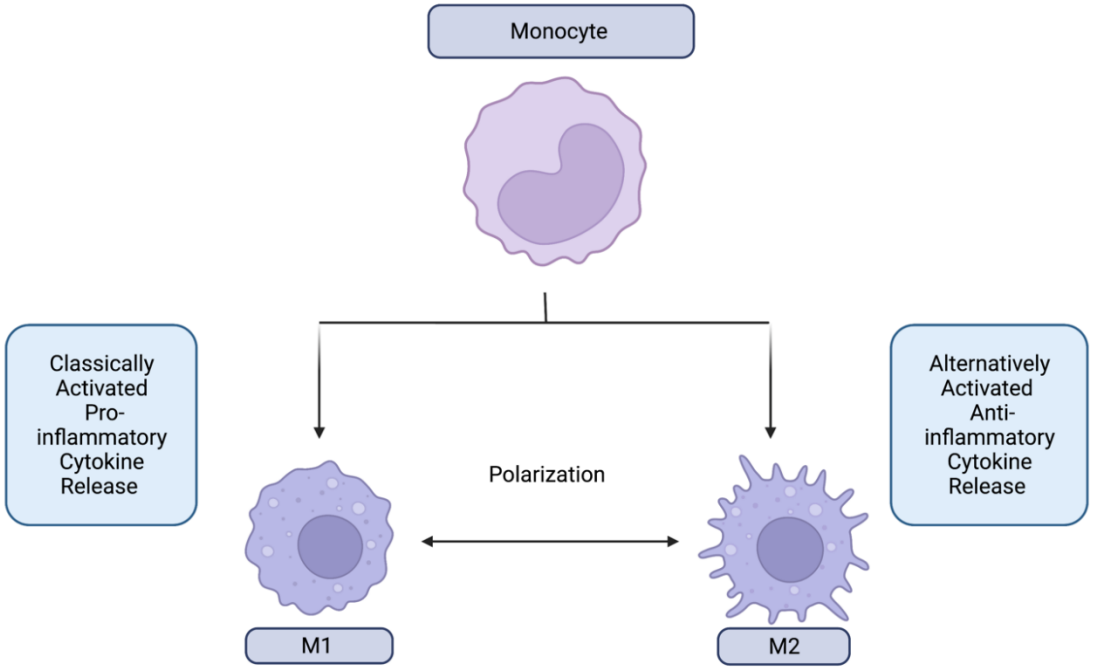

Figure 1. M1 and M2 Macrophage Phenotypes. Macrophages are derived from myeloid cell lineages. The M1 type is classically activated and respond to environmental stimuli, such as bacterial exposures. During polarization secretes pro-inflammatory cytokine releases, including TNF- α. The M2 phenotype is alternatively activated and respond to alternative environmental stimuli to releases anti-inflammatory cytokines including IL-10. Created with Biorender.com.

As mentioned previously, a major activator of the innate immune response and signaling for macrophage polarization to the M1 phenotype is the bacterial component, LPS. LPS is located on the outer membrane of Gram-negative bacteria, such as *Escherichia coli* (Miller et al., 2005), and is used later in this investigation as a non-specific immune activator. Innate immune activation occurs through pathogen-associated molecular patterns (PAMP) and ligation of pattern recognition receptors (PRR) (Janeway et al., 2002). PAMPs are recognized by PRRs, one of which is the family of toll-like receptors (TLRs). TLR recognition of PAMP signals activates signaling pathways and the production of pro-inflammatory cytokines involved in the innate immune response (Schnare et al., 2001), including activating macrophages for phagocytosis (Mathison et al., 1993).

LPS is a PAMP that activates the innate immune system through the ligation of TLR-4. On M1 macrophages, a pro-inflammatory signaling cascade of events begins with PAMP recognition. This causes a conformational change in the TLR which recruits the adapter protein, MyD88. Recruitment of MyD88 leads to a phosphorylation event in the Iκκ complex. Phosphorylation of the Iκκ complex then results in I_KB releasing from the transcriptional regulator, nuclear factor-kappa b (NF-κB). Once released from I_KB, NF-κB is free to translocate to the nucleus and become a transcriptional activator turning on pro-inflammatory cytokine production, such as TNF-α (Siebenlist et al., 1994; Trentin et al., 2017; Liu et al., 2020) (Figure 2).

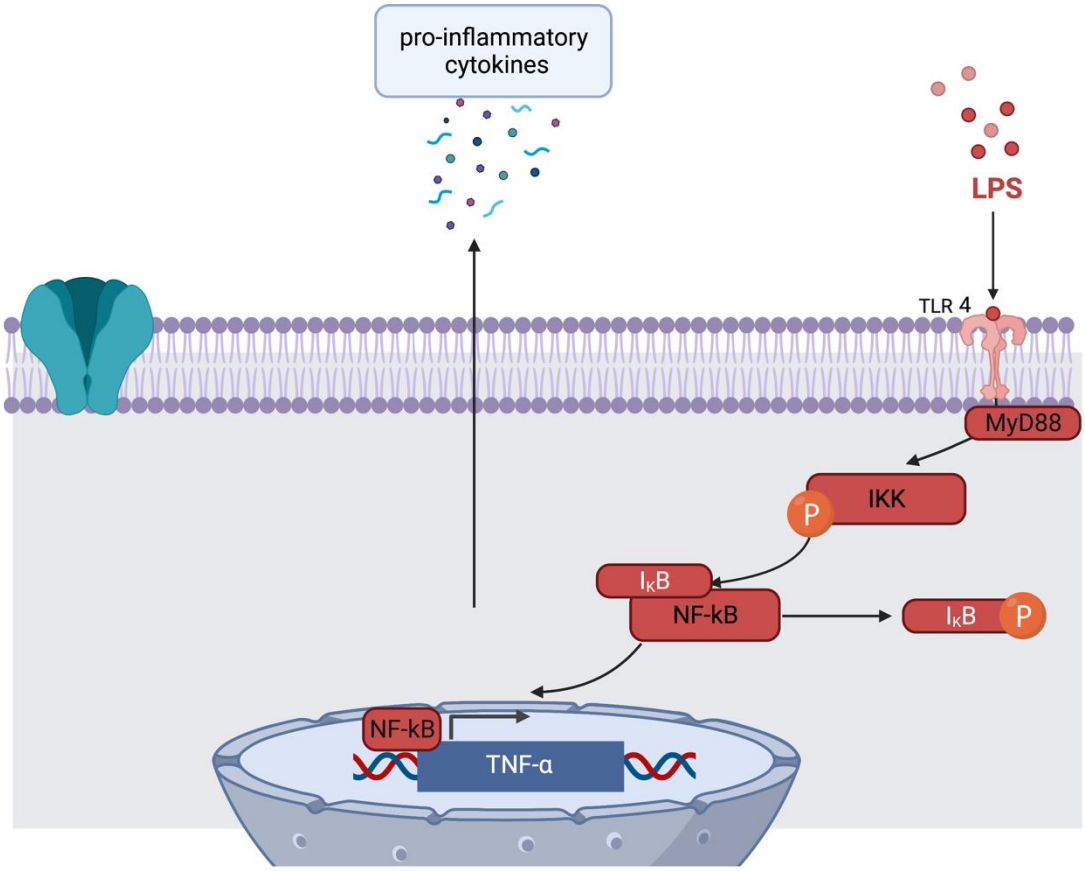

Figure 2: Activation of Inflammation via TLR-4 Pathway. In the M1 macrophage phenotype, there is an upregulation of pro-inflammatory cytokines initiated by TLR-4 recognition of LPS. This leads to MyD88 recruitment and phosphorylation in the IKK complex, releasing I_KB and allowing NF-κB to translocate into the nucleus and activate transcription of pro-inflammatory cytokines. Created with Biorender.com.

Alternatively, after the biological threat has been alleviated, pro-inflammatory cytokines are downregulated through a series of receptor-mediated signaling events from increased abundance of these proinflammatory cytokines, specifically TNF-α. In addition to the downregulation of TNF-α, the upregulation of anti-inflammatory cytokines is seen in the M2 phenotype (Palacios et al., 2015; Chu et al., 1991). One specific anti-inflammatory cytokine of interest is interleukin-10 (IL-10) which is released through cytokine receptor signaling and activation of the Janus Kinase (JAK)/ signal transducer and activation of transcription 3 (STAT3) signaling pathways (Riley et al., 1999; Wehinger et al., 1996). In this signaling cascade, the increased presence of TNF-α binding to the cytokine receptor results in downstream signaling through the JAK/STAT3 pathway inhibiting TNF-α production while upregulating the production of anti-inflammatory cytokines such as IL-10, regulated through a separate cytokine receptor (Figure 3). Additionally, the production of the anti-inflammatory cytokine IL-10 down-regulates the production of the pro-inflammatory cytokine TNF-α stimulated by the presence of LPS (Meraz et al., 1996; Rodig et al., 1998). In studies where the STAT3 genes were knocked out, macrophages failed to increase expression of IL-10 and its downstream signaling effects. A vital effect in this research includes IL-10's ability to downregulate the production of TNF-α in the LPS-induced murine macrophage cell line, RAW 267.4 cells. (Riley et al., 1999). This homeostatic regulation results in polarization of the macrophage phenotype from the M1 pro-inflammatory phenotype to the M2 anti-inflammatory phenotype (Figure 3).

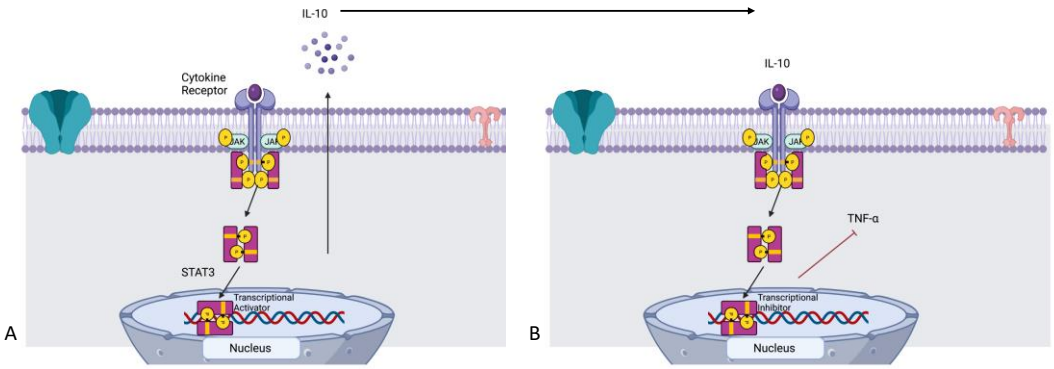

Figure 3. **Polarization of Macrophages from the M1 to the M2 Phenotype. A.** Using the JAK/STAT3 protein signaling pathways, macrophages respond to increased levels of pro-inflammatory cytokines to produce IL-10, an anti-inflammatory cytokine and marker of the M2 phenotype. **B.** In response to increased IL-10 production M2 macrophages down-regulate the production of TNF-α, a cytokine marker for the M1 phenotype. This results in a polarization of the M1 to the M2 phenotype. Created with Biorender.com.

One molecular mechanism behind this polarization of the M1 and M2 phenotypes can be traced back to the alpha 7 nicotinic acetylcholine receptor (α7 nAChR) found on the cell surface of macrophages. The signaling pathway of this receptor is involved in the cholinergic anti-inflammatory pathway (CAP). A recent study on the CAP demonstrated that when RAW 264.7 macrophage cells were stimulated by LPS, it led to the differentiation of macrophages to the M1 phenotype, which is expected (Tan et al., 2022). Researchers then stimulated the α7 nAChR of these activated cells with the agonist PNU282987, which polarized the M1 to the M2 phenotype and its resulting anti-inflammatory effects. Thus, these data strongly support the role of α7 nAChR in the molecular mechanism of macrophage plasticity. To further understand the complexity of this receptor and its role in mitigating LPS-induced inflammation in the presence of an iHg co-exposure, it is vital to describe the CAP and its regulators in more detail.

The CAP functions to attenuate the immune system's pro-inflammatory response to pathogens via dual processes (Figure 4). The most well understood mechanism is to decrease the translocation of the transcriptional factor NF-κB. When NF-κB enters the nucleus, it functions as a transcriptional activator resulting in the upregulation of TNF-α production (Natarajan et al., 1998). Additionally, this signaling pathway initiates phosphorylation events in the JAK/STAT3 signaling pathway (DeJonge et al., 2005; Zhao et al., 2019). The CAP is initiated by stimulation of the vagus nerve, cranial nerve ten (CNX), and effector T-cells because both aid in release of acetylcholine (ACh). ACh then activates the CAP pathway by stimulating the α7 nAChR with calcium ions and resulting in formation of inositol triphosphate (IP3) acting to drive the processes behind the JAK/STAT3 pathway. Once activated by ACh, the CAP results in the aforementioned

downstream effects on cytokine production, including the upregulation of IL-10 through STAT3 signaling (Riley et al, 1999), and downregulation of TNF-α (Borovikova et al., 2000).

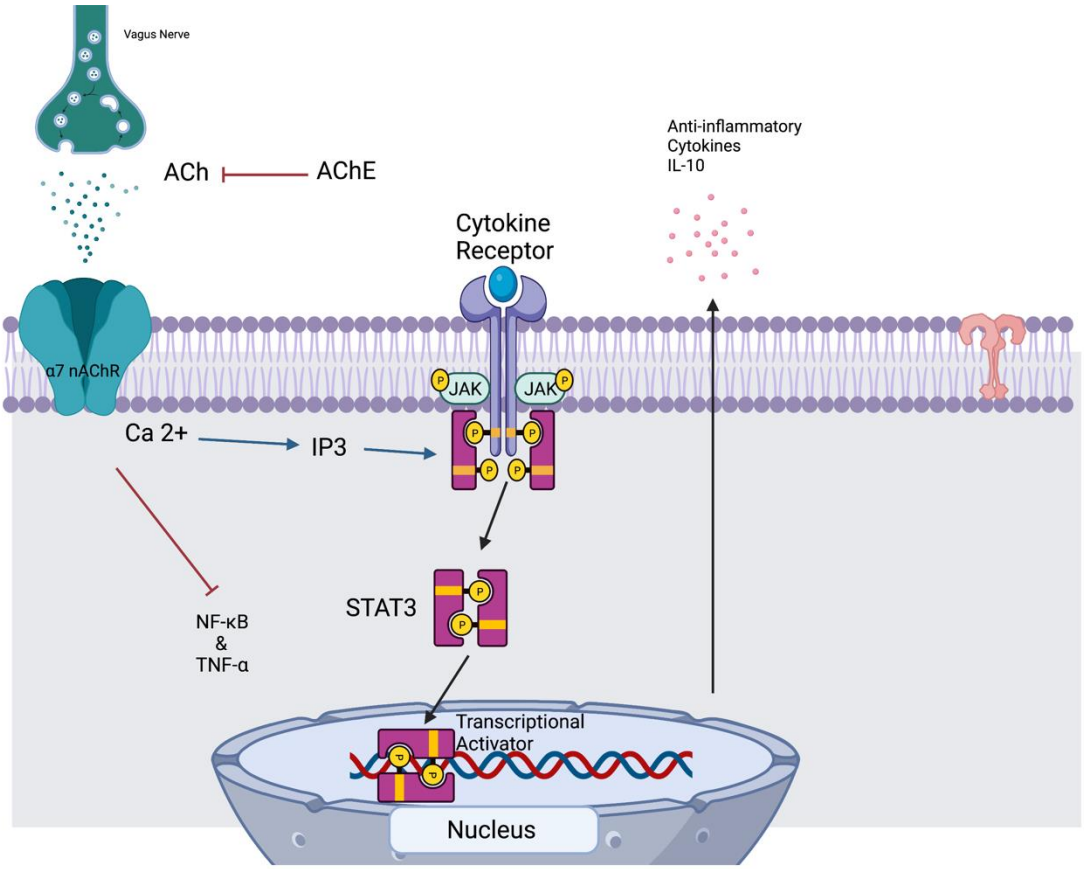

Figure 4. The Cholinergic Anti-inflammatory Pathway. The cholinergic anti-inflammatory pathway functions via dual process. The stimulation of the vagus nerve results in the production of ACh and the ligand-receptor relationship of the of the α7 nAChR. This includes calcium activation of IP3 and transcriptional activation of IL-10. First this interaction results in inability of NF-κB to translocate into the nucleus and upregulate the pro-inflammatory cytokine, TNF-α. This also

activates the calcium signaling of IP3 and transcriptional activation of IL-10 through the JAK/STAT3 signaling pathways. Created with Biorender.com.

A less studied regulator of the CAP is the enzyme acetylcholinesterase (AChE) and the focus of this investigation. AChE is a serine protease responsible for the rapid hydrolysis of ACh into acetate and choline, which are inactive metabolites. This gives the enzyme regulatory ability by directly hydrolyzing ACh, an activator of the α7 nAChR and the substrate for this enzyme (Pavlov et al., 2009) (Figure 4). Theoretically, hydrolysis of ACh would result in the inhibition of all downstream signaling involving the α7 nAChR and its involvement in the CAP. This would also offer a viable explanation for the results by Gardner, et al, (2009) which described an unopposed pro-inflammatory response with a co-exposure of primary human immune cells to mercury and LPS.

Mercury has been well-documented as a neurotoxicant (Basu et al., 2007; Silbergeld et al.,2005; Wiess et al., 2002). Alternatively, mercury has also been recognized as an immunotoxicant (Fournie et al., 2001; Gardner et al., 2010a, Gardner et al., 2010b; Silva, 2004). Studies have demonstrated that mercury dysregulates the immune system only when combined with an immune-activating event. For example, immune dysregulation with mercury is observed when mercury is combined with additional pathogens such as Coxsackievirus B3, the causative agent for autoimmune myocarditis (Nyland et al., 2012), or other pathogens which non-specifically engage the innate immune response (Fournie et al., 2001). This upregulated inflammatory response is not observed with lower doses of mercury alone (Figure 5) (Fournie et al., 2001; Gardner et al., 2009, Gardner et al., 2010b; Nyland et al., 2012, Silbergeld et al., 2005), but rather only with an immune-activating co-exposure.

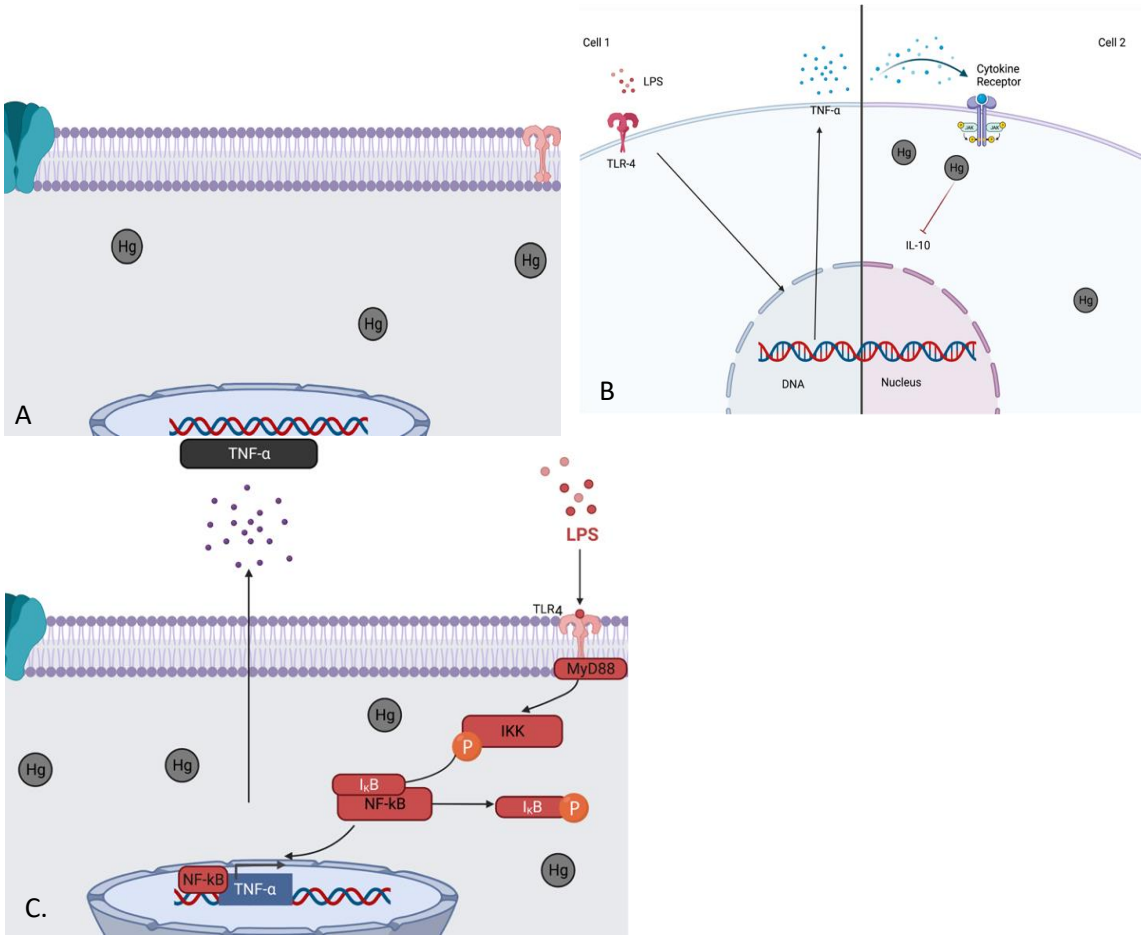

Figure 5. Low-dose Mercury Exposure. A. In the event of mercury exposure at 200nM alone, the TLR-4 pathway for inflammation is not activated and various cytokines like IL-10 are not released. **B.** When LPS activates the TLR-4 pathway the resulting TNF-α eventually binds to cytokine receptors to release anti-inflammatory cytokines, like IL-10. This increased production of IL-10 then results in signaling to inhibit further production of TNF-α. **C**. When the TLR-4 pathway is activated in the presence of low doses of iHg, there is an increase in pro-inflammatory cytokines such as TNF-α and an absence of anti-inflammatory cytokines like IL-10. Created with Biorender.com.

Previous studies have demonstrated that low doses of mercury coupled with activation of the TLR-4 pathway by LPS induces an unopposed pro-inflammatory response and M1 phenotype polarization. Evaluations of pro-inflammatory cytokines in the presence of this co-exposure demonstrated an increase in the release of these cytokines, such as TNF-α, without the simultaneous upregulation of anti-inflammatory cytokines, such as IL-10, typically observed in the absence of mercury. This observation of the resulting cytokine dysregulation was defined as an unopposed pro-inflammatory response (Gardner et al., 2009).

Although it is well-supported that these signaling pathways have become dysregulated, the mechanisms by which mercury modulates the pathways remain unclear. Previous work has demonstrated that low doses of mercury, along with activation of the TLR-4 pathway using LPS induces upregulation of pro-inflammatory cytokines with an absence of anti-inflammatory cytokines (Gardner et al., 2009). While these studies demonstrated the impacts of sub-cytotoxic mercury in the presence of an immune activator on the release of pro-inflammatory cytokines, gene expression was not examined. This project begins to explore the dysregulation of the signaling pathways of these cytokines (Figure 5) in a co-exposure scenario, specifically LPS and mercuric chloride.

This project aims to develop a technique to evaluate the role of AChE enzymatic function in the cytokine dysregulation resultant from co-exposure to nanomolar concentrations of mercury utilizing a model of bacterial infection. I established an *in vitro* assay testing for effects of mercury on AChE. The *in vitro* enzyme kinetics analysis was modeled from Ellman's method (Ellman et al., 1961) and those found in Dhanasekaran et al. (2005). This method utilizes the substrate, acetylthiocholine chloride, which reacts with

Ellman's reagent, 5,5-Dithio-bis(2-nitrobenzoic acid) (DTNB) into 2-nitrobenzoate-5-mercatothiocholine and 5-thio-nitrobezoate (TNB). TNB yields a yellow color in this coupled reaction and is measured at 412nm via spectrophotometry (Figure 6). The use of acetylthiocholine chloride was chosen over acetylthiocholine iodide used in Dhanasekaran et al. (2005) to keep the *in vitro* system as simple as possible. Since mercuric chloride already has chlorine in it, using acetylthiocholine chloride minimizes the number of additional chemical elements in the system whereas acetylthiocholine iodide would have added a chemical element.

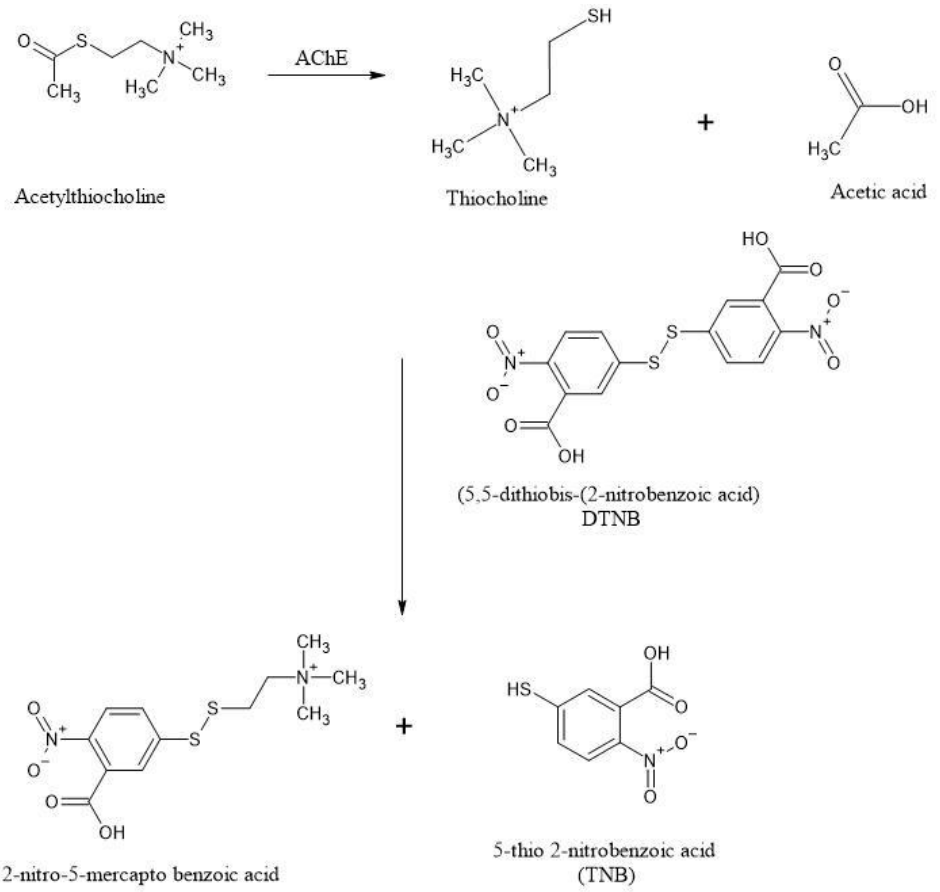

Figure 6. Chemical Mechanism of Ellman's Method. Acetylthiocholine and acetylcholinesterase (AChE) from *Electrophorus electricus* were used to establish the reaction to yield thiocholine. Thiocholine reacts with Ellman's reagent, DTNB, to yield a mixed disulfide and 5-thio-2-nitrobenzoic acid (TNB) which gives off a yellow color. The color is then measured at 412nm via spectrophotometry. Prior to performing this technique, we tested that the coupled reaction was balanced and that any baseline reaction with $HgCl_2$ was negligible. Created with ChemSketch.

The research conducted with both mercury and AChE to establish a relationship between mercury exposure and the observed pro-inflammatory response is particularly challenging at physiologically relevant mercury doses due to the dynamics of each component separately. AChE's shape is not conserved amongst different organisms, and different mercury concentrations have been shown to alter the function of this enzyme in various organisms differentially. Changes to enzymatic function in different organisms have been seen in millimolar concentrations of mercury (Frasco et al., 2007) and have not yet been observed in lower (more physiologically relevant and sub-cytotoxic) concentrations such as the nanomolar range. Further complicating this system is the unusual nature of the active site of AChE. The AChE active site has been predicted with microsecond molecular dynamic simulations and consists of a deep gorge that is difficult to access, with residue variations throughout the radius of the active site (Cheng et al., 2017. Studies have suggested the presence of a separate binding and release site on AChE, with the deep gorge responsible for substrate selectivity and multiple exit sites for the products leaving the reaction (Bennion et al., 2015).

Methods and Materials

RAW 246.7 Cell Culture

All products were purchased from Sigma Aldrich unless otherwise stated. Murine macrophages (RAW 246.7, ATCC) were grown in supplemented Dulbecco's Modification of Eagle's Medium at 37 °C with 5% CO_2 in 25 cm^2 tissue culture-treated flasks. The supplemented media included 10% fetal bovine serum, and 1% penicillin (10,000 I.U./mL)/streptomycin (10,000 ug/mL). Cells were grown as adherent cultures until approximately 80% confluency prior to passage (Figure 7).

At passage, a single culture was separated into flasks for experimental condition growth with or without 20 nM $HgCl_2$ and LPS (50 ng/mL). Cells were split at passage, allowed to grow undisturbed for two days (one day prior to 80% confluency), and then growth media was replaced with supplemented media containing the different exposure combinations. The experimental combinations consisted of $HgCl_2$/LPS, (+/+), $HgCl_2$ alone (+/-), LPS alone (-/+), negative control (-/-). Cells were grown for an additional 24 hours before harvesting for cell density and viability quantification and collection of cell culture supernatants and cell pellets for later analyses. Independent experiments were performed in triplicate.

Cell Density and Viability Quantification

Cell density and cell viability were assessed by hemocytometer and 0.4% trypan blue using standard methods.

Cell Pellet Collection

The cell pellet was collected by centrifugation and resuspended in approximately 200 µL of phosphate-buffered saline. In addition to the cell pellet, supernatant from each treatment group was also frozen at -20 °C for future analysis.

In Vitro AChE Assay

AChE activity was measured based on Ellman's method (Ellman et al., 1961). AChE from *Electrophorus electricus* was purchased from Sigma-Aldrich. This was used to hydrolyze the substrate acetylthiocholine chloride, which reacts with Ellman's reagent, 5,5-Dithio-bis(2-nitrobenzoic acid) (DTNB) into 2-nitrobenzoate-5-mercatothiocholine and 5-thio-nitrobezoate (TNB). TNB yields a yellow color in this coupled reaction measured at 412nm via spectrophotometry (Figure 6). Reactions were established in the presence or absence of $HgCl_2$ (10 or 20nM final concentration), AChE (0.625 U/mL), in 50mM Tris-HCl buffer at 8.0 pH and incubated for 15 minutes at 25℃. Acetylthiocholine chloride was added to initiate the reaction and absorbance measurements were collected every 10 seconds for 90 seconds via VISIONlite™ software. Experiments were performed in triplicate.

Statistical analysis

Statistical differences among groups were assessed with 2-way ANOVA.

Gene expression analysis

Total RNA was isolated from RAW 267.4 cell homogenates using TRIzol® reagent (Invitrogen) as per the manufacturer's recommended protocol, and the concentration was determined with a Nanodrop 2000 spectrophotometer (Thermo Scientific, Waltham, MA, USA). A cDNA library was constructed using reverse transcriptase PCR according to the

manufacturer's protocol (Versa kit, Invitrogen). Gene sequences specific for AChE, TNF-α, and the HPRT reference gene were amplified using primers designed with Snap Gene software 3.0 (San Diego, CA, USA) and synthesized by Fisher Scientific (Table 1). Gene products of interest were amplified by PCR and separated with gel electrophoresis. Band intensity was utilized for qualitative relative gene expression analysis.

Table 1. Primers

	Forward	Reverse
AChE	AAT CGA GTT CAT CTT TGG GCT CCC CC	CCA GTG CAC CAT GTA GGA GCT CCA
TNF-α	AGT GAC AAG CCT GTA GCC	AGG TTG ACT TTC TCC TGG
HPRT	TCA GTC AAC GGG GGA CAT AA	AAA GCA GTT ACT AAT GTT TCT TGG T

Results

My thesis focuses on the potential role of AChE in mercury dysregulation of immune signaling. Since this exact mechanism, especially at the nanomolar mercury concentration range, has never been examined, I began with the simplest system to examine the effects of mercury on AChE enzyme function. The *in vitro* assay of the enzymatic function of AChE was performed using acetylthiocholine substrate concentrations of 125µM to 2,500µM. The data were first plotted for analysis with a Michaelis-Menton curve (Figure 8). The inverse of substrate and V_o concentrations were then used for the Lineweaver-Burk plot for calculation of the V_{max} and K_m (Table 2). The Lineweaver-Burk analysis then allowed for analysis of AChE inhibition by $HgCl_2$ (Figure 9). Low-dose mercury (both 10 and 20nM) inhibited AChE activity. Specifically, the V_{max} was 1.24 x 10^{-4} µmoles/min for AChE alone, 9.44 x 10^{-5} µmoles/min with 10nM mercury, 9.24 x 10^{-4} µmoles/min with 20nM mercury. These data suggest that low dose exposure to mercury results in uncompetitive inhibition of AChE. Both the V_{max} and K_m decreased with low concentrations of iHg (Table 2), while the Lineweaver-Burk plot's slope under all three experimental conditions remained the same. These results support the presence of 20 nM mercury as an uncompetitive inhibitor, which is truly an uncommon occurrence.

Table 2: K_m and V_{max} Values for AChE with $HgCl_2$ Exposure.

Concentration of $HgCl_2$ Exposure	V_{max} (µmoles/min)	K_m (µmoles)
Control	1.24×10^{-4}	6.25×10^{-5}
10 nM	9.44×10^{-5}	4.71×10^{-5}
20 nM	9.25×10^{-5}	4.63×10^{-5}

After utilizing this very simple *in vitro* enzyme kinetics system to examine the effects of low concentrations of $HgCl_2$ on AChE function, I increased the complexity of the system by utilizing cell culture cells that had been treated with 20nM $HgCl_2$ in culture as the AChE source.

We first needed to verify that under our proposed cell culture conditions, with low dose mercury exposure in the presence or absence of LPS, there was no overt induced cell death. Since high dose mercury exposure is known to be cytotoxic, this was an important first step. For consistency with the *in vitro* enzyme kinetics assays discussed previously, we decreased the 200nM from previous studies to 20nM. None of the treatment conditions used had a significant effect on cell viability or cell density of RAW murine macrophages (Figure 7).

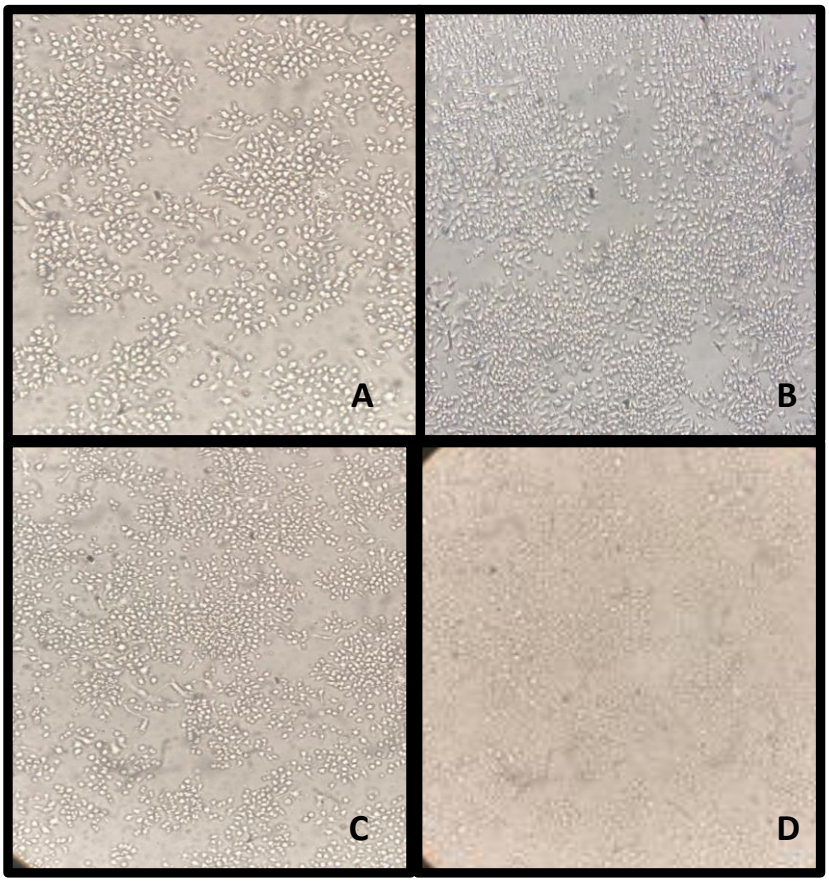

Figure 7. RAW 267.4 Macrophages Micrograph. Measurements of cell confluency for harvesting were performed when each group reached approximately 80% in supplemented media. **A.** Experimental grouping of 20nM $HgCl_2$ and LPS. **B.** Experimental grouping of $HgCl_2$ only. **C. Experimental** grouping of LPS only. **D.** Negative Control using supplemented media only.

Finally, preliminary analyses of mercury modulation of gene expression were conducted to test the hypothesis that mercury induces transcript-level changes in AChE in cell culture, potentially as a result of the induced inhibition of the enzyme. The preliminary data suggest that, indeed, 20nM $HgCl_2$ along with the immune activator LPS, alters gene expression in 20 nM exposures of $HgCl_2$ in AChE gene expression (Figures 10).

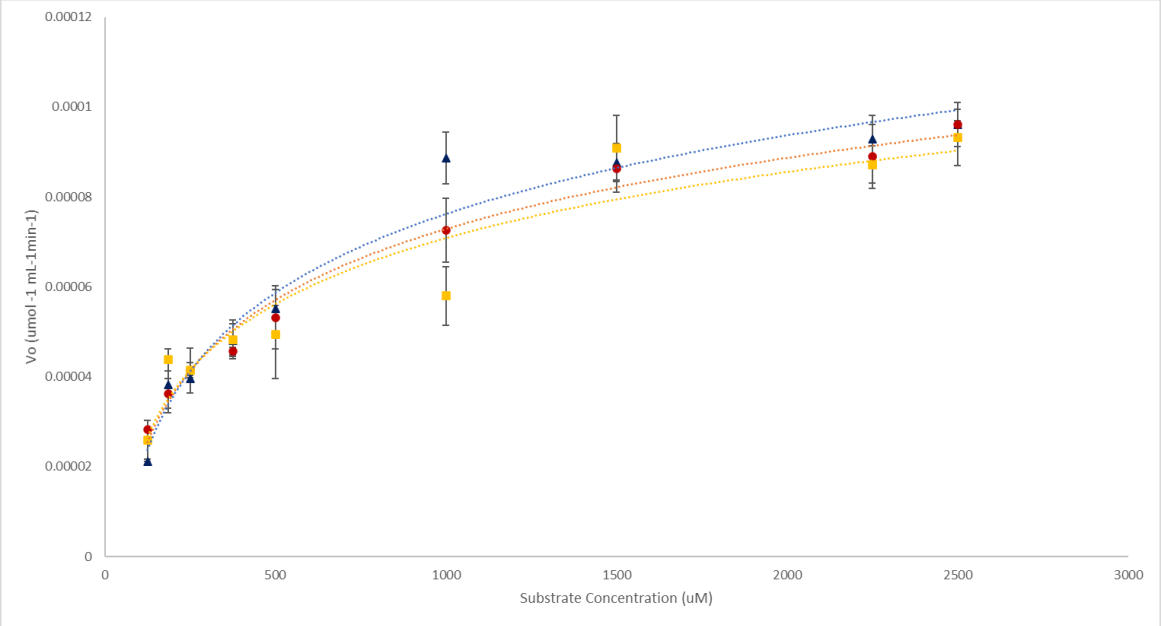

Figure 8. Michaelis-Menten Plot of Mercuric Chloride Effects on Acetylcholinesterase. The *in vitro* assay observed AChE activity with Ellman's method using DTNB over 90 seconds. The control group is represented by blue triangles and has an R2 value of 0.9636. Exposure to 10 nM of $HgCl_2$ is represented by red circles and has an R2 value of 0.9848. Exposure to 20 nM $HgCl_2$ is represented by yellow squares and has an R2 value of 0.9105.

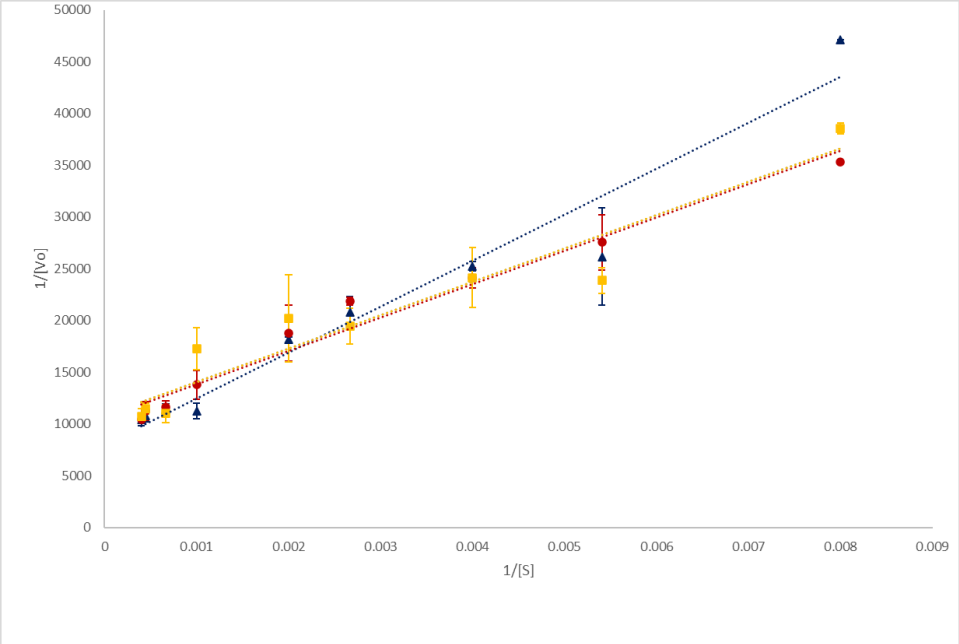

Figure 9. Lineweaver-Burk Plot of Mercuric Chloride Effects on Acetylcholinesterase. The *in vitro* assay observed AChE activity with Ellman's method using DTNB over 90 seconds. This used the inverse of substrate concentrations and Vo. Vo. The control group is represented by blue triangles and has an R2 value of 0.9537 and linear equation of y=3E+06x+8041. Exposure to 10 nM total assay concentration of $HgCl_2$ is represented by red circles and has an R2 value of 0.9726 and a linear equation of y=3E+06x+10594. Exposure to total assay concentration of 20 nM $HgCl_2$ is represented by yellow squares and has an R2 value of 0.922 and a linear equation of y=3E+06x+10810.

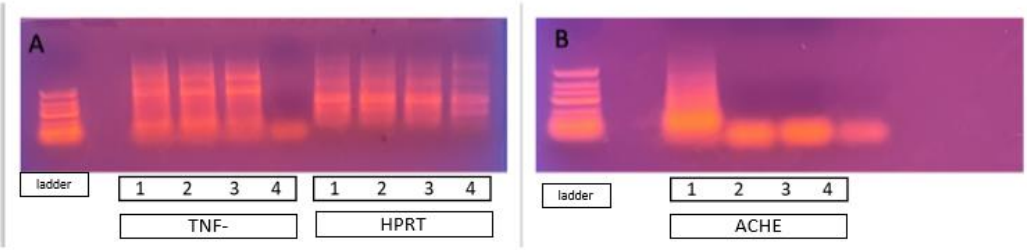

Figure 10. Relative Expression of TNF-α and ACHE in $HgCl_2$ Exposed RAW 264.7 Macrophages. PCR of TNF-α and ACHE expression from RAW 264.7 macrophages exposed to 20nM $HgCl_2$. Column one represents mercury and LPS co-exposure. Column two is mercury alone, three is LPS alone, and four is negative control.

Discussion

Previous studies demonstrate the ability of mercury to insight an unopposed pro-inflammatory response through the upregulation of pro-inflammatory cytokines, such as TNF-α and the downregulation of anti-inflammatory cytokines, such as IL-10. Notably, this occurs with mercury exposures in the nanomolar range, but only when combined with LPS (Gardner et al., 2009). LPS activates the innate immune response simulating the exposure of a Gram-negative bacterial infection through the TLR-4 pathway. This upregulated pro-inflammatory response and decreased anti-inflammatory response is not observed with these same exposures of mercury alone (Fournie et al., 2001; Gardner et al., 2009, Gardner, et al., 2010b; Nyland et al., 2012, Silbergeld et al., 2005.), but rather only with the immune-activating co-exposure. It's important to note that while this response is well-documented, the molecular mechanisms of these findings remain unclear. My data indicates that when the TLR-4 pathway is activated and low doses of $HgCl_2$ are introduced to the system, the response of the immune system differs from low concentration exposures of iHg or LPS alone. These findings in conjunction with the supported dysregulation of AChE offer a model for further studies into the CAP and the enzyme, AChE, as a feasible explanation.

The study of enzyme kinetics, like those performed with AChE, is vital to understanding biological systems and how they become dysregulated. The function of an enzyme is to lower activation energy by stabilizing the transition state and increase the rate of reactions occurring within these systems. In this process the enzyme binds to a substrate and results in the enzyme-substrate complex, before yielding a new product or products while the enzyme remains unchanged. The process of this product formation from enzyme

activity would happen in the absence of enzymatic activity, though not fast enough to be biologically advantageous.

In the case of uncompetitive inhibition, the inhibitor binds to the enzyme and enhances the binding of its substrate. This results in the reduction of K_m, or the concentration of substrate where the reaction occurs at half of its maximum velocity. Furthermore, it results in the creation of a substrate-inhibitor-enzyme complex which forms the product at a slower rate (Cornish-Bowden, 1986). This results in a decreased V_{max} (the maximum rate of enzyme of enzyme catalyzed reaction) in addition to the decrease in K_m (Figure 11).

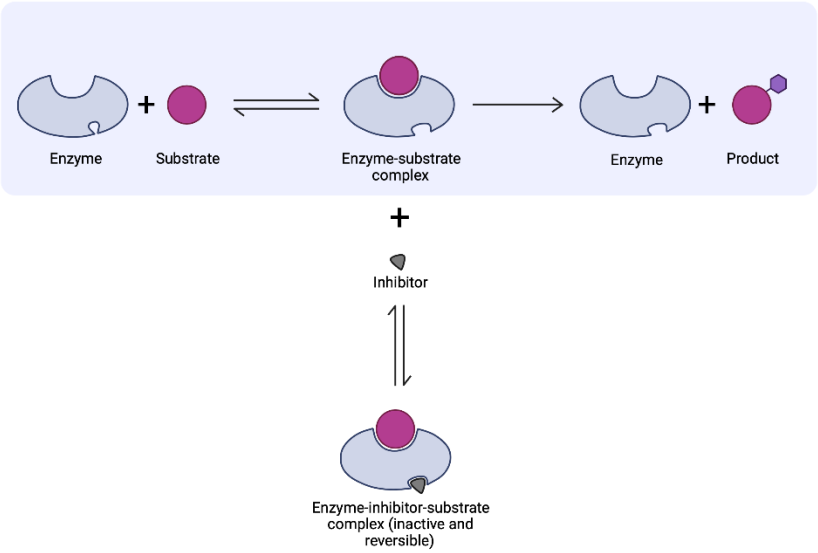

Figure 11. Uncompetitive inhibition. To best lower activation energy, enzymes bind to their substrate, forming an enzyme-substrate complex. This complex then stabilizes the transition state as the reaction proceeds forward to result in a new product, while the structure of the enzyme remains unchanged. In the case of uncompetitive inhibition, the formation of the enzyme-inhibitor-substrate complex results in a decreased rate of product formation. Created with Biorender.com.

True uncompetitive enzyme inhibition is very rare and thus there are limited published studies examining the impacts to gene expression from uncompetitive inhibition of the enzyme. Theoretically, the temporary decrease in enzymatic function would result in the upregulation in the enzyme expression by the cell as a compensatory mechanism to return the system back to homeostatic balance.

The uncompetitive inhibition of AChE observed in this study becomes more complicated to analyze when we include the traditional methods of testing for AChE

function with mercury exposures. In studies examining the potential impacts to enzymatic dysfunction with $HgCl_2$, the mercury concentrations tested tend to be in higher doses than we use and are thus not physiologically and environmentally relevant, that is, up to the millimolar range (Frasco et al., 2007). In keeping with other studies examining the differential effects of high versus low mercury exposures, the mechanism of enzyme inhibition has the potential to be different if the amount of mercury present is high enough to flood and inhibit the active sites in the deep gorge of AChE and thus affect the substrate selectivity of the enzyme. In the event the low dose exposures of $HgCl_2$ are interacting with what Frasco, et al., (2007) described as the side door or back door of the enzyme exit site and inhibiting the hydrolysis of ACh, the inhibition would be uncompetitive, and thus reversable. This can explain why there is no change in cell viability or density (Figure 7).

Using PCR and gel electrophoresis to analyze gene expression patterns in our treated cell cultures, I found that AChE gene expression was upregulated when macrophages were co-exposed to 20nM concentrations of $HgCl_2$ and LPS. This effect was not found with either LPS or mercury alone (Figure 10). Interestingly, with this extremely low dose mercury exposure, we found that in all treatment groups (co-exposure to mercury and LPS, mercury alone, and LPS alone), TNF-α expression was upregulated compared to the negative control (Figure 10).

The difference in response leading to the activation of the CAP has implications in treating an array of different diseases such as multiple sclerosis, stroke (Han et al., 2017), wound healing, cancer, cardiovascular, respiratory, digestive, and orthopedic disease (Fujii et al., 2017). In these diseases, understanding the relationship between low dose $HgCl_2$ and AChE activity as it pertains to these disease phenotypes, offers viable mechanism for future

pharmaceutical targets in these diseases not previously considered. By considering AChE as point of manipulation, the M1 and M2 phenotypes can be altered through this enzymatic function, and thus potentially modulating the disease phenotype, severity, or symptoms.

Previous studies have extensively examined the stimulation of the vagus nerve resulting in the upregulation of ACh (Borovikova, 2000). Also considered is the activity of the α7 nAChR in response to agonist and antagonist activity (Tan, et al., 2022). For clarification of the function of the CAP, one could consider the impact of nicotine on cell signaling. Nicotine reacts the α7 nAChR to result in the same downstream signaling as when the receptor is activated with ACh. Multiple studies support the presence of nicotine causing the polarization of macrophages from the M1 to the M2 phenotype (Yuan et al., 2014; Wongtrakool et al., 2012). This suggests the same effects would be inhibited if ACh was hydrolyzed by an increase in AChE gene expression as a response to a temporary inhibition prior to interaction with the α7 nAChR.

This interaction also supports the importance of this preliminary study of AChE as a major regulator of the system. In the event ACh is unable to activate the α7 nAChR signaling cascade as is observed with nicotine, it would alter all subsequent downstream reactions. When noting the upregulation of ACHE in the presence of a co-exposure (Figure 10) as a mechanism to overcome a temporary mercury inhibition (Figure 9), it is feasible that the increased expression would result in over-production of the enzyme. This over production would result in the upregulation of TNF-α after downregulation of IL-10 (Figure 5). The resulting outcome is then the unopposed pro-inflammatory response through AChE, evidenced in previous studies (Figure 12).

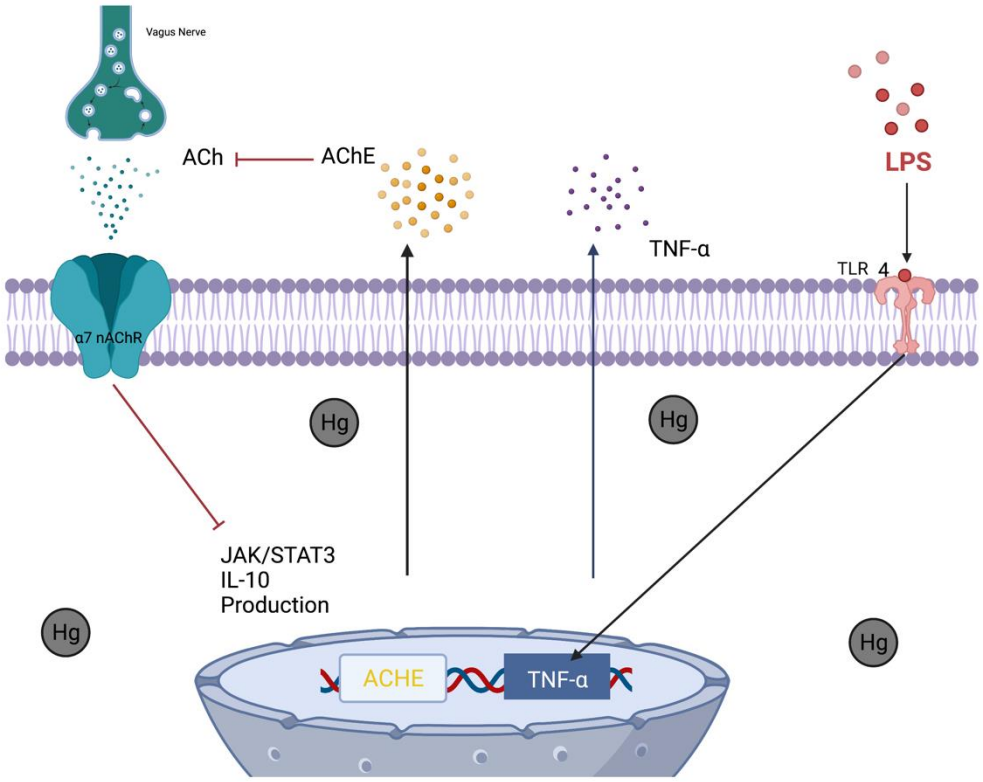

Figure 12. Mercury's Effect on Acetylcholinesterase Resulting in an Unopposed Inflammatory Response. The presence of LPS results in activation of the TLR-4 pathway and release of proinflammatory cytokines such as TNF-α. The presence of low concentrations of mercury results in reversible uncompetitive inhibition of AChE activity and upregulation of AChE gene expression. This offers an explanation for the increase in TNF-α and decrease in IL-10 through inhibition of the CAP. Created with Biorender.com.

Future Studies

RAW 267.4 AChE Kinetics

The importance of a more comprehensive examination of the enzyme kinetics in the RAW 267.4 cell line of macrophages cannot be understated. In a closed system consisting of enzyme and substrate alone with $HgCl_2$ acting as the inhibitor, I demonstrated the uncompetitive inhibition of AChE, which is reversible. When this *in vitro* system's complexity is increased by examining the system in macrophages, the gene expression of AChE is increased. This is likely a mechanism to return homeostatic balance resulting in overexpression of AChE. When AChE is overexpressed, it would theoretically result in the inhibition of the CAP's usage of the IL-10 production pathway and downstream events including the unopposed pro-inflammatory response.

Zebrafish

Future studies will utilize the *in vivo* model organism, zebrafish (*Danio rerio*). Zebrafish are well supported as model organisms in both toxicological and immunological studies (Richetti et al., 2011; Novoa et al., 2009; Ho et al., 2013). Both zebrafish and RAW 264.7 cells have TLR-4 pathways which can be activated in the presence of doses of LPS (Kim et al., 2018, Novoa et al., 2009, Ko et al., 2019) with studied pathways being conserved between organisms. Furthermore, the protagonist enzyme, butyrylcholinesterase, is not present in zebrafish (Linney et al., 2004) supporting the use of zebrafish as a viable *in vivo* model. In this model, zebrafish embryos will be used with methylmercury to examine the effects of mercury on AChE activity in living, whole animal models.

References

Basu, N., Scheuhammer, A.M., Evans, R.D., O'Brien, M., & Chan, H.M. (2007) Cholinesterase and monoamine oxidase activity in relation to mercury levels in the cerebral cortex of wild river otters. *Human and Experimental Toxicology,* 26, 213-220.

Bennion, B.J., Essiz, S.G. Lau, E.Y., Fattebert, J.L., Emigh, A., & Lightstone, F.C. (2015) A wrench in the works of human acetylcholinesterase: Soman induced conformational changes revealed by molecular dynamics simulations. *PLOS One*, 10, e0121092.

Borovikova, L.V., Ivanova, S., Zhang, M., Yang, H., Botchkina, I.G., Watkins, L.R., Wang, H., Abumrad, N., Eaton, J.W., & Tracy, K.J. (2000). Vagus nerve stimulation attenuates the systemic inflammatory response to endotoxin. *Nature,* 405(6785), 458-62.

Berlin, M., Zalups, R.K., & Fowler, B.A. (2007). Mercury. In G.F. Nordberg, B.A. Fowler, M. Nordberg, and L.T. Friberg (Eds.), *Handbook on the Toxicology of Metals* (3rd ed., Chapter 33). Elsevier.

Cheng, S., Song, W., & Yuan, X. (2017). Gorge motions of acetylcholinesterase revealed by microsecond molecular dynamics simulations. *Scientific Reports,* 7, 3219.

Chu, C.Q., Field, M., Feldman, M., & Maini, R.N. (1991). Localization of tumor necrosis factor alpha in synovial tissues and the cartilage-pannus junction in patients with rheumatoid arthritis. *Arthritis and Rheumatology,* 34, 1125-32.

Crompton, P., Ventura, A.M., de Souza, J.M., Santos, E., Strickland, G.T., & Silbergeld, E. (2002). Assessment of mercury exposure and malaria in a Brazilian Amazon riverine community. *Environmental Research,* 90(2), 69–7.

Cornish-Bowden, A. (1986). Why is uncompetitive inhibition so rare?: A possible explanation, with implications for the design of drugs and pesticides. *FEBS Letters*. 203(1),3-6.

DeJonge, W.J., Esmerij, V.D.Z., The, F.O., Frans, O.T., Bijilsma, M.F., & VanWesterloo, D. (2005). Stimulation of the vagus nerve attenuates macrophage activation by activating the JAK2-STAT3 signaling pathway. *Natural Immunology,* 6(8), 844-851.

Dhanasekaran, D., Perumal, P., & Palayan, M. (2005) In-vitro screening for acetylcholinesterase enzyme inhibition potential and antioxidant activity of extracts of Ipomoea aquatica forsk: Therapeutic lead for Alzheimer's disease. *Journal of Applied Pharmaceutical Science,* 5(02), 012-016.

Ellman, G.L., Courtney, K.D., Andres Jr., V., & Feather-Stone, R.M. (1961) A new and rapid colorimetric determination of acetylcholinesterase activity. *Biochemical Pharmacology*, 7, 88–95.

Fournie, G.J., Mas, M., Cautain, B., Savignac, M., Subra, J.F., Pelietier, L., Saoudi, A., Lagrangge, D., Calise, M., & Druet, P. (2001). Induction of autoimmunity through bystander effects. Lessons from immunological disorders induced by heavy metals. *Journal of Autoimmunity*, 16(3), 319-328.

Frasco, M.F., Colletier, J., Weik, M., Carvalho, F., Guilhermino, L., Stojan, J., & Fournier, D. (2007). Mechanisms of cholinesterase inhibition by inorganic mercury. *FEBS Journal,* 274, 1849-1861.

Fujii, A.T., Mashimo, M., Moriwaki, Y., Misawa, H., Ono, S., Horiguchi, K., & Kawashimia, K. (2017). Physiological functions of the cholinergic system in immune cells. *Journal of Pharmacological Science*, 134, 1-21.

Gardner, R.M. Nyland, J.F., Evans, S.E., Wang, S.E., Doyle, K.M., Crainiceanu, C., & Silbergeld, E.K. (2009). Mercury induces an unopposed inflammatory response in human peripheral blood mononuclear cells i*n vitro*. *Environmental Health Perspectives*, 117(12), 1932-1938.

Gardner, R.M., Nyland, J.F., Silva, I.A., Ventura, A.M., de Souza, J.M., & Silbergeld, E.K. (2010a). Mercury exposure, serum antinuclear/antinuclear antibodies, and serum cytokine levels in mining populations in Amazonian Brazil: A cross-sectional study. *Environmental Research,* 110, 345-354.

Gardner, R.M., Nyland, J.F., & Silbergeld, E.K. (2010b). Differential immunotoxic effects of inorganic and organic mercury species *in vitro*. *Toxicology Letters,* 198, 182-190.

Han, B., Li, X., & Hao, J. (2017). The cholinergic anti-inflammatory pathway: An innovative treatment for neurological diseases. *Neuroscience and Biobehavioral Reviews*, 77, 358-368.

Ho, N.Y., Yang, L., Legardi, J. Armant, O., Takamiya, M, Rastegar, S., & Strahle, U. (2013). Gene responses in the central nervous system of zebrafish embryos exposed

to the neurotoxicant methylmercury. *Environmental Science and Technology*, 47, 3316-3325.

Houserová, P., Kubáňa, V., & Jiljí, S. (2007). Total mercury and mercury species in birds and fish in an aquatic ecosystem in the Czech Republic. *Environmental Pollution,* 145, 185-194.

Hightower, J.M., & Moore, D. (2003). Mercury levels in high-end consumers of fish. *Environmental Health Perspectives*, 111, 604–60

Janeway Jr., C.A., & Medzhitov, R. (2002). Innate immune recognition. *Annual Review of Immunology*, 20, 197-216.

Kim, E., Kim, S., Ye, B., Kim, J., Ko, S., Lee, W.W., Kim, K., Coi, I., Jung, W., & Heo, S. (2018). Anti-inflammatory effect of apo-9'-fucoxanthinone via inhibition of MAPKs and NF-kB signaling pathway in LPS-stimulated RAW 264.7 macrophages and zebrafish model. *Internal Immunopharmacology,* 59, 339-349.

Ko, E., Heo, S., Cho, S., Lee, W.W., Kim, S., Yang, H., Ahn, G., Cha, S., Kwon, S., Jeong, M.S., Lee, K.P., Jeon, Y., & Kim, K. (2019). 3-Bromo-5(ethoxymethyl)-1,2-benzenediol inhibits LPS-induced pro-inflammatory responses by preventing ROS production and downregulating NF-kB i*n vitro* and in a zebrafish model. *Internal Immunopharmacology,* 67, 98-105.

Linney, E., Upchurch, L., & Donerly, S. (2004). Zebrafish as a neurotoxicological model. *Neurotoxicology and Teratology,* 36, 79-718.

Li, Y., & Cai, Y. (2013). Progress in the study of mercury methylation and demethylation in aquatic environments. *China Science Bulletin,* 58, 177-185.

Liu, Y.L.E., Xia, Y., Kong, X., Guo, M.S.S., Yu, A.X.D., Zheng, B.Z.Y., Mak, S., Xu, M.L. & Tsim, K.W.K. (2020). Interacting with α7 nAChR is a new mechanism for AChE to enhance the inflammatory response in macrophages. *Acta Parmaceutica Sinica B,* 10(10), 1926-1942.

Mathison, J., Wolfson, E., Steinemann, S., Tobias, P., & Ulevitch, R. (1993). Lipopolysaccharide (LPS) recognition in macrophages. Participation of LPS-binding protein and CD14 in LPS-induced adaptation in rabbit peritoneal exudate macrophages. *The Journal of Clinical Investigation,* 92(4), 2053–2059.

Meraz, M.A., White, J.M., Sheehan, K.C.F., Bach, E.A., Rodig, S.J., Dighe, A.S., Kaplan, D.H., Riley., J.K., Greenhund, A.C., Campbell, D., Carver-Moore, K., DuBois., R.N., Clark, R., Arguet, M., & Schreiber, R.D. (1996) Targeted disruption of the STAT1 gene in mice reveals unexpected physiological specificity in the JAK-STAT signaling pathway. *Cell,* 84, 431-442.

Miller, S., Ernst, R., & Bader, M. (2005). LPS, TLR4 and infectious disease diversity. *Nature Reviews Microbiology,* 3, 36–46.

Natarajan K., Manna S.K., Chaturvedi M.M., & Aggarwal B.B. (1998). Protein tyrosine kinase inhibitors block tumor necrosis factor-induced activation of nuclear factor-κB, Degradation of IκBα, nuclear translocation of p65, and subsequent gene expression. *Archives of Biochemistry and Biophysics,* 352(1), 59-70.

Nathan, C.F., Murray, H.W., Wiebe, M.E., & Rubin, B.Y. (1983). Identification of interferon-gamma as the lymphokine that activates human macrophage oxidative metabolism and antimicrobial activity. *Journal of Experimental Medicine,* 158, 670-689.

National Research Council. (2000). *Toxicological Effects of Methylmercury*. Washington, DC: The National Academies Press.

Novoa, B., Bowman, T.V., Zon, L., & Figueras, A. (2009). LPS response and tolerance in the zebrafish (*Danio rerio*). *Fish & Shellfish Immunology,* 26, 326-331.

Nyland, J.F., Fairweather, D., Shirley, D.L., Davis, S.E., Rose, N.R., & Silbergeld, E.K. (2012). Low-dose inorganic mercury increases severity and frequency of chronic coxsackievirus-induced autoimmune myocarditis in mice. *Toxicological Sciences,* 125(1), 134-143.

Palacios B.S., Estrada-Capetillo, L., Izquierdo, E., Criado, G., Nieto, C., Municio, C., Gonzalez-Alvaro, I., Sanchez-Mateos, P., Pablos, J.L., Corbi, A.L., & Puig-Kröger, A. (2015). Macrophages from the synovium of active rheumatoid arthritis exhibit an activin A-dependent pro-inflammatory profile. *Journal of Immunology,* 235(3), 515-26.

Pavlov, V.A., Parrish, W.R., Rosas-Ballina, M., Ochani, M., Puerta, M., Ochani, K., Chavan, S., Al-Abed, Y., & Tracey, K. (2009). Brain acetylcholinesterase activity controls systemic cytokine levels through cholinergic anti-inflammatory pathway. *Brain, Behavior, and Immunity,* 23, 41-45.

Regiera, N., Larrasa, F., Garcia Bravoa, A., Ungureanu, V., Amouroux, D., & Cosio, C. (2013). Mercury bioaccumulation in the aquatic plant *Elodea nuttallii* in the field and in microcosm: Accumulation in shoots from the water might involve copper transporters. *Chemosphere*, 90, 595-602.

Research Triangle Institute; Agency for Toxic Substances and Disease Registry. (1999). *Toxicological Profile for Mercury.* Atlanta: US Department of Health and Human Services.

Richetti, S.K., Rosemberg, D.B., Ventura-Lima, J., Monserrat, J.M., Bogo, M.R., & Bononan, C.D. (2011). Acetylcholinesterase activity and antioxidant capacity of zebrafish brain is altered by heavy metal exposure. *NeuroToxicology*, 32, 116-122.

Riley, J.K., Takeda, K., Akira, S., & Schreiber, R.D. (1999). Interleukin-10 receptor signaling through the JAK-STAT pathway. *Journal of Biological Chemistry*, 274(23), 16513-16521.

Rodig, S.J., Meraz, M.A., White, J.M., Lampe, P.A., Riley, J.K., Arthur, C.D., King, K.L., Sheehan, K.C., Yin, L., Pennica, D., Johnson, E.M., & Schreiber, R.D. (1998). Disruption of the JAK1 gene demonstrates obligatory and nonredundant roles of the JAKS in cytokine-induced biological responses. *Cell*, 93, 373-383.

Rothenberg, S.E., Yu, X., Liu, J., Biasini, F.J., Hong, C., Jiang, X., Nong, Y., Cheng, Y., & Korrick, S.A. (2016). Maternal methylmercury exposure through rice ingestion and offspring neurodevelopment: a prospective cohort study. *International Journal of Hygiene and Environmental Health*, 8, 832-842.

Schnare, M., Barton, G., Holt, A. Agnieszka Czopik, H., Takeda, K., Akira, S., & Medzhitov, R. (2001). Toll-like receptors control activation of adaptive immune responses. *Nature Immunology*, 2, 947–950.

Siebenlist, U., Franzoso, G., & Brown, K. (1994). Structure, regulation and function of NF-kappa B. *Annual Review of Cell and Developmental Biology*, 10, 405-455.

Silbergeld, E.K., Silva, I.A., & Nyland, J.F. (2005). Mercury and autoimmunity: implications for occupational and environmental health. *Toxicology and Applied Pharmacology*, 207, s282-s292.

Silva, I.A., Nyland, J.F., Gorman, A., Perisse, A., Ventura, A.M., Santos, E.C., deSouza, J.M., Burek, C.L., Rose, N.R., & Silbergeld, E.K. (2004). Mercury exposure, malaria, and serum antinuclear/antinucleolar antibodies in Amazon populations in Brazil: a cross-sectional study. *Environmental Health*, 3**,** 11.

Skinner, K., Wright, N., & Porter-Goff, E. (2007). Mercury uptake and accumulation by four species of aquatic plants. *Environmental Pollution*, 145, 234-237.

Stein, M., Keshav, S., Harris, N., & Gordon, S. (1992). Interleukin 4 potently enhances murine macrophage mannose receptor activity: a marker of alternative immunologic macrophage activation. *Journal of Exploratory Medicine*, 176, 287-92.

Tan, Y., Chu, Z., Shan, H., Zhangsun, D., Zhu, X., & Luo, S. (2022). Inflammation regulation via an agonist and antagonists of α7 nicotinic acetylcholine receptors in RAW 264.7 macrophages. *Marine Drugs*, 20(3), 200-218.

Treinin, M., Papke, R.L., Nizri, E., Ben-David, Y., Mizrachi, T., & Brenner T. (2017). Role of the $\alpha 7$ nicotinic acetylcholine receptor and RIC-3 in the cholinergic anti-inflammatory pathway. *Central Nervous System Agents Medicinal Chemistry,* 17(2), 90-99.

Tuhy, M., Rohovec, J., Matouskova, S., Mihaljevic, M., Kribeck, B., Vanek, A., Marpani, B., Gottlicher, J., Steininger, R., & Majzlan, J. (2020). The potential wildfire effects on mercury remobilization from topsoils and biomass in a smelter-polluted semi-arid area. *Chemosphere,* 247, 125972.

U.S. Environmental Protection Agency. Basic information about mercury. Retrieved March 28, 2022a, from https://www.epa.gov/mercury/basic-information-about-mercury.

U.S. Environmental Protection Agency. How people are exposed to mercury. Retrieved March 28, 2022b, from https://www.epa.gov/mercury/how-people-are-exposed-mercury#metallicmercury.

Wehinger, J., Gouilleux, F., Groner, F., Groner, B., Finke, J., Mertelsmann, R., & Weber-Nordt, R.M. (1996). IL-19 induces DNA binding activity of three STAT proteins (Stat1, Stat3, Stat5) and their distinct combinational assembly in the promotors of selected genes. *FEBS Letters,* 194, 365-370.

Weiss, B., Clarkson, T.W., & Simon, W. (2002). Silent latency periods in methylmercury poisoning and in neurodegenerative disease. *Environmental Health Perspectives,* 110, 851-854.

Wongtrakool, C., Grooms, K., Ping, X., Rivera, H., Ward, J., Roser-Page, S., Roman, J., Brown, L.A., & Gauthier, T.W. (2012). In utero nicotine exposure promotes activation in neonatal mouse alveolar macrophages. *Nature*, 72, 147-53.

Yaun, F., Fu, X., Shi, H., Chen, G., Dong, P., & Zhang, W. (2014). Induction of murine macrophage M2 polarization by cigarette smoke extract via JAK2/STAT3 pathway. *PLOS One*, 9(9), e107063.

Zhao, X., Yu., Z., Lv, Z., Meng, L., Yuan, S., & Fu, Z. (2019). Activation of α7 nicotinic acetylcholine receptors (α7 nAChR) promotes the protective autophagy in LPS-induced acute lung injury (ALI) in vitro and in vivo. *Inflammation*, 42, 2236-2245.